Long-range order by crucial non-linear effects in Heisenberg models

1991 J. Phys.: Condens. Matter 3 5861

(http://iopscience.iop.org/0953-8984/3/31/009)

J. Phys.: Condens. Matter 3 (1991) 5861–5873. Printed in the UK

Long-range order by crucial non-linear effects in Heisenberg models

E Rastelli, S Sedazzari and A Tassi
Dipartimento di Fisica dell'Universitá 43100 Parma, Italy

Received 31 July 1990, in final form 11 Febuary 1991

Abstract. Linear spin wave theory usually provides reliable indications about the absence of long-range order (LRO) in Heisenberg models. Here we study the equilibrium configuration of the three-dimensional Heisenberg model with competitive interactions in the neighbourhood of the phase boundary between the ferromagnetic and helical phases where linear spin wave theory suggests the absence of LRO caused by a *soft* $k_{\perp}^{4}$ behaviour of the spin wave energy in the long wavelength limit. To assess the reliability of this indication we have studied the two-magnon bound states which exist below the two-magnon band over the whole Brillouin zone in all cases where exact results assure the absence of LRO. We did not find any bound states for sufficiently small wavevectors on the ferro–helix transition line. So we have performed a controlled low-temperature calculation beyond the linear approximation for the spin wave spectrum and the order parameter. We have proved that non-linear contributions restore LRO in contrast with previous speculations.

1. Introduction

The lowest lying excitation in the Heisenberg model is the single spin wave (SW) when long-range order (LRO) is present [1]. This is the case of the three-dimensional Heisenberg model with nearest neighbour (NN) ferromagnetic interaction for which linear SW theory provides the *exact* low temperature thermodynamics [2]. The scenario is completely different in one and two dimensions where the LRO is absent as is required in both the Landau argument [3] and the Mermin and Wagner theorem [4]. In both cases the SW mode is still an exact eigenstate of the model when the NN interaction is ferromagnetic but it is no longer the lowest one. Two-magnon bound states exist below the two-magnon band for all wavevectors, whereas in the three-dimensional model no bound states are found below the two-magnon band, for sufficiently small wavevectors [5]. Even for layered structures, where the in-plane exchange coupling J is greater than the inter-plane coupling J' no bound states below the two-magnon band exist in the neighbourhood of the zone centre for any $J' \neq 0$. Notice that in all such examples the existence of the bound states for all wavevectors is concomitant with a catastrophic occupation number of long wavelength magnons that causes the failure of LRO.

For this reason it is suggested that the presence of the two-magnon bound states below the two-magnon band until zero wavevector should signal the absence of LRO. This suggestion provides a useful test for the possible absence of LRO indicated by approximated arguments.

0953-8984/91/315861+13$03.50

Here we consider the Heisenberg model with in-plane competitive interactions up to third neighbours, the NN one being ferromagnetic, while only NN spins on adjacent layers are coupled. This model shows a rich phase diagram in the parameter space with two different helix phases (H_1, H_2) and two colinear phases (AF, F) [6–8]. This model, called the 3N-model, is expected to be disordered on the H_1–H_2 and F–H phase boundary until zero temperature on the basis of the linear SW approximation because a divergent spin deviation from its saturation value is noticed at any finite temperature by the existence of soft lines [9] in the SW spectrum on the H_1–H_2 line and by a peculiar softening of the SW spectrum at long wavelengths [7] on the F–H line.

Here we calculate the two-magnon bound state energy only on the F–H phase boundary. Notice that the model on this line shows a two-dimensional-like behaviour in the linear SW approximation [7]. Indeed in the small wavevector limit the magnon energy shows a $k_\perp^4$ behaviour, $k_\perp$ being the projection of the wavevector on the basal plane. Such behaviour leads to a divergent number of spin deviations in spite of the three-dimensional nature of the model. If this fact is genuine evidence of the absence of LRO, bound states below the two-magnon band until the zone centre should be expected. On the contrary we find that the bound states exhibit a three-dimensional behaviour which usually occurs when LRO is present. A careful criticism of the simple SW argument suggests that the scenario is totally different from that expected on the basis of the linear SW approximation.

The format of this paper is the following: in section 2 the two-magnon bound state energy is evaluated on the F–H phase boundary. In section 3 we prove the existence of LRO on the F–H line taking into account the non-linear contribution at the lowest order in $1/S$ and temperature. In section 4 we give the summary and concluding remarks.

2. Two-magnon bound states for the 3N model

Non-conventional ground state configurations in Heisenberg models, that is non-colinear and non-helical configurations, are believed to be possible in particular regions of the parameter space corresponding to suitable exchange competition [10]. The onset of these unorthodox phases has been ascribed to zero point quantum fluctuations that are responsible, for instance, for the spin liquid phase in Heisenberg antiferromagnets in the neighbourhood of the transition between Néel and helix configurations. A strong indication of this is provided by a divergent spin reduction arising from soft lines in the magnon excitation spectrum [10]. Other examples exist where the critical dimensionality seems to be lowered from $D = 3$ to $D = 2$ for Heisenberg models. In particular we focus on the 3N Heisenberg model with a ferromagnetic NN interaction on the F–H phase boundary [7] where the magnon dispersion curve shows a $k_\perp^4$ behaviour at long wavelengths instead of the usual $k_\perp^2$ behaviour. In this case linear SW theory leads to a divergent occupation number which causes a divergent demagnetization at any finite temperature. This could imply the existence at any finite temperature of a spin liquid phase in the neighbourhood of the F–H transition line.

Let us give a brief sketch of the argument supporting this conclusion. The Hamiltonian we consider reads

$$H = -\sum_{\alpha} J_\alpha \sum_{i,\delta_\alpha} S_i \cdot S_{i+\delta_\alpha} - J' \sum_{i,\delta'} S_i \cdot S_{i+\delta'} \tag{2.1}$$

where δ_α and δ' are vectors joining site i with its neighbours of the αth shell and with its out-of-plane NN, respectively. Here the NN in-plane J_1 and the out-of-plane J' exchange couplings are positive, while the next nearest neighbours (NNN) J_2 and the third nearest neighbours (TNN) J_3 coupling can have either sign. If J_2 and/or J_3 are negative, the competition between exchange interactions can lead to helical states. On the other hand, there is no competition due to J': the spins in each basal plane have identical orientations. The SW energy in the ferromagnetic configuration reads

$$\hbar\omega_k = 8J_1S\{1 - \tfrac{1}{2}(\cos ak_x + \cos ak_y) + j_2(1 - \cos ak_x \cos ak_y) + j_3[1 - \tfrac{1}{2}(\cos 2ak_x + \cos 2ak_y)] + \tfrac{1}{2}j'(1 - \cos ck_z)\} \tag{2.2}$$

where $j_\alpha = J_\alpha/J_1$, $j' = J'/J_1$, a and c are the in-plane and out-of-plane lattice constants. As one can see the coefficient of $k_\perp^2$ vanishes on the F–H phase boundary given by $1 + 2j_2 + 4j_3 = 0$, $j_3 < 0$ [6].

The expectation value of the magnetization evaluated by means of linear SW approximation is affected by a divergent number of spin deviations that leads to the t–j_3 phase diagram shown in figure 1 for $j_2 = 0$ and $j' = 0.01$. The reduced temperature is $t = k_BT/2J_1S$. The qualitative features of the phase diagram do not change along the F–H phase boundary. Clearly we refer to the range where the zero temperature F–H phase transition is continuous. This is assured on a large portion of this phase boundary even if this phase transition becomes first order in the neighbourhood of the F–H–AF triple point owing to long wavelength quantum fluctuations [8].

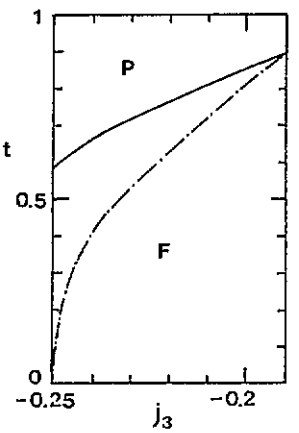

Figure 1. t–j_3 phase diagram of the 3N model for $j_2 = 0$, $j_3 > -\frac{1}{4}$ and $j' = 0.01$ as obtained either from linear SW approximation (chain curve) or from HF approximation (full curve). F and P mean ferromagnetic and paramagnetic phase, respectively.

Here we search for the two-magnon bound states because we expect that their existence below the two-magnon band until the zone centre should be a reliable test for the two-dimensional-like behaviour suggested by the linear SW theory on the F–H line. Let us consider the two-magnon eigenstate $|q\rangle$ for the bosonic equivalent Hamiltonian obtained from the Heisenberg Hamiltonian (2.1) by the Dyson–Maleev transformation [2].

$$|q\rangle = \sum_k f_q(k) a_{k_1}^\dagger a_{k_2}^\dagger |0\rangle \tag{2.3}$$

where

$$k_1 = \tfrac{1}{2}q + k \qquad k_2 = \tfrac{1}{2}q - k \tag{2.4}$$

and $f_q(k)$ satisfies the following equation

$$\hbar\left(\omega - \omega_{\frac{1}{2}q+k} - \omega_{\frac{1}{2}q-k}\right) f_q(k) = -\sum_\alpha z_\alpha J_\alpha \frac{1}{N}\sum_{k'}\left(\gamma^{(\alpha)}_{k+k'} + \gamma^{(\alpha)}_{k-k'} - \gamma^{(\alpha)}_{\frac{1}{2}q+k} - \gamma^{(\alpha)}_{\frac{1}{2}q-k}\right) f_q(k') \tag{2.5}$$

where z_α is the coordination number of the αth shell of neighbours.

$$\gamma^{(\alpha)}_k = \frac{1}{z_\alpha}\sum_{\delta_\alpha} e^{i\mathbf{k}\cdot\delta_\alpha} \tag{2.6}$$

$$\hbar\omega = E - E_0 \tag{2.7}$$

where E is the eigenvalue of the eigenstate $|q\rangle$ and E_0 is the energy of the ferromagnetic ground state $|0\rangle$. The solution of equation (2.5) is obtained by looking for the zeros of the following determinantal equation

$$\det\left|\delta_{m,n} - \frac{\hat{\jmath}_m}{2S}\left(D_m \cos\tfrac{1}{2}q_n - D_{m,n}\right)\right| = 0 \tag{2.8}$$

where

$$D_m = \frac{1}{N}\sum_k \frac{\cos k_m}{\epsilon - \sum_{l=1}^{7}\hat{\jmath}_l\left(1 - \cos\tfrac{1}{2}q_l\cos k_l\right)} \tag{2.9}$$

$$D_{m,n} = D_{n,m} = \frac{1}{N}\sum_k \frac{\cos k_m \cos k_n}{\epsilon - \sum_{l=1}^{7}\hat{\jmath}_l\left(1 - \cos\tfrac{1}{2}q_l\cos k_l\right)} \tag{2.10}$$

with

$$\epsilon = \frac{\hbar\omega}{8J_1 S} \tag{2.11}$$

$$k_1 = ak_y \qquad k_2 = ak_x \qquad k_3 = a(k_x + k_y) \qquad k_4 = a(k_x - k_y)$$
$$k_5 = 2ak_y \qquad k_6 = 2ak_x \qquad k_7 = ck_z \tag{2.12}$$

$$\hat{\jmath}_1 = \hat{\jmath}_2 = 1 \qquad \hat{\jmath}_3 = \hat{\jmath}_4 = j_2 \qquad \hat{\jmath}_5 = \hat{\jmath}_6 = j_3 \qquad \hat{\jmath}_7 = j'. \tag{2.13}$$

The explicit forms of the D_ms and $D_{m,n}$s are given in the appendix. The evaluation of the bound state energy has been performed by solving numerically equation (2.8) for $S = \frac{1}{2}$. We have found bound states for selected values of the exchange parameter on the F–H phase boundary. Explicit calculations have been done for the $(1,1,0)$ and $(1,0,0)$ directions. In figure 2(a) we show the bound state dispersion curve for $j_2 = 0$, $j_3 = -\frac{1}{4}$, $j' = 0.01$ along the $(1,1,0)$ direction. In figure 2(b) we show the same for $j' = 0.001$. As one can see two bound states appear in the $(1,1,0)$ direction. Notice the peculiar q^4 dependence of the lower bound of the two-magnon band (continuous curve) in the long wavelength region. Figure 2(c) gives the bound state along the $(1,1,0)$ direction at the triple point F–H_1–H_2. In the $(1,0,0)$ direction only one bound state exists as shown in figure 2(d) for $j_2 = 0$, $j_3 = -\frac{1}{4}$ and $j' = 0.001$. We have found that the bound state existence region is narrowed by increasing S and/or j'.

In this section we have found the bound state on the F–H transition line and we have numerically shown and analytically checked that no bound states exist for sufficiently long wavelengths. Such a fact is usually a good support for the existence of LRO, whereas linear SW theory suggests no LRO on the F–H phase boundary.

$j' = 0.001$. As one can see two bound states appear in the $(1,1,0)$ direction. Notice the peculiar q^4 dependence of the lower bound of the two-magnon band (continuous curve) in the long wavelength region. Figure 2(c) gives the bound state along the $(1,1,0)$ direction at the triple point F–H_1–H_2. In the $(1,0,0)$ direction only one bound state exists as shown in figure 2(d) for $j_2 = 0$, $j_3 = -\frac{1}{4}$ and $j' = 0.001$. We have found that the bound state existence region is narrowed by increasing S and/or j'.

In this section we have found the bound state on the F–H transition line and we have numerically shown and analytically checked that no bound states exist for sufficiently long wavelengths. Such a fact is usually a good support for the existence of LRO, whereas linear SW theory suggests no LRO on the F–H phase boundary.

3. Spin wave renormalization and LRO supported by non-linear effects

The contrasting indications about LRO for the 3N model on the F–H phase boundary obtained from linear SW theory and from the features of the two-magnon bound states in the long wavelength region call for a controlled approach to account for the effect of non-linear contributions on the SW energy and the spontaneous magnetization. We evaluate the self-energy $\Sigma_k^{(1)}$ at the lowest order in $1/S$ and temperature, that is the Hartree–Fock (HF) approximation.

$$\Sigma_k^{(1)} = -\sum_\alpha \frac{2z_\alpha J_\alpha}{\hbar N} \sum_q \left(1 + \gamma_{k-q}^{(\alpha)} - \gamma_k^{(\alpha)} - \gamma_q^{(\alpha)}\right) n_q. \tag{3.1}$$

The renormalized SW spectrum within the HF approximation reads

$$\hbar\omega_k^{(1)} = \hbar\left(\omega_k + \Sigma_k^{(1)}\right) = \sum_\alpha 8J_\alpha S(1-\rho_\alpha)(1-\gamma_k^{(\alpha)}) + 4J'S(1-\rho')(1-\gamma_k') \tag{3.2}$$

where

$$\rho_\alpha = \frac{1}{NS}\sum_q (1-\gamma_q^{(\alpha)}) n_q \tag{3.3}$$

$$\rho' = \frac{1}{NS}\sum_q (1-\gamma_q') n_q. \tag{3.4}$$

The reduced spontaneous magnetization σ is

$$\sigma = \frac{\langle S_i^\zeta\rangle}{S} = 1 - \frac{1}{NS}\sum_k \langle a_k^\dagger a_k\rangle \tag{3.5}$$

where

$$\langle a_k^\dagger a_k\rangle = -\frac{1}{\pi}\int_{-\infty}^{\infty} d\omega \frac{1}{e^{\beta\hbar\omega}-1} \operatorname{Im} G_k^{(1)}(\omega + i\eta) \tag{3.6}$$

where Im means imaginary part. The limit $\eta \to 0^+$ has to be performed. The Green function is given by

$$G_k^{(1)}(\omega) = \frac{1}{\omega - \omega_k - \Sigma_k^{(1)}}. \tag{3.7}$$

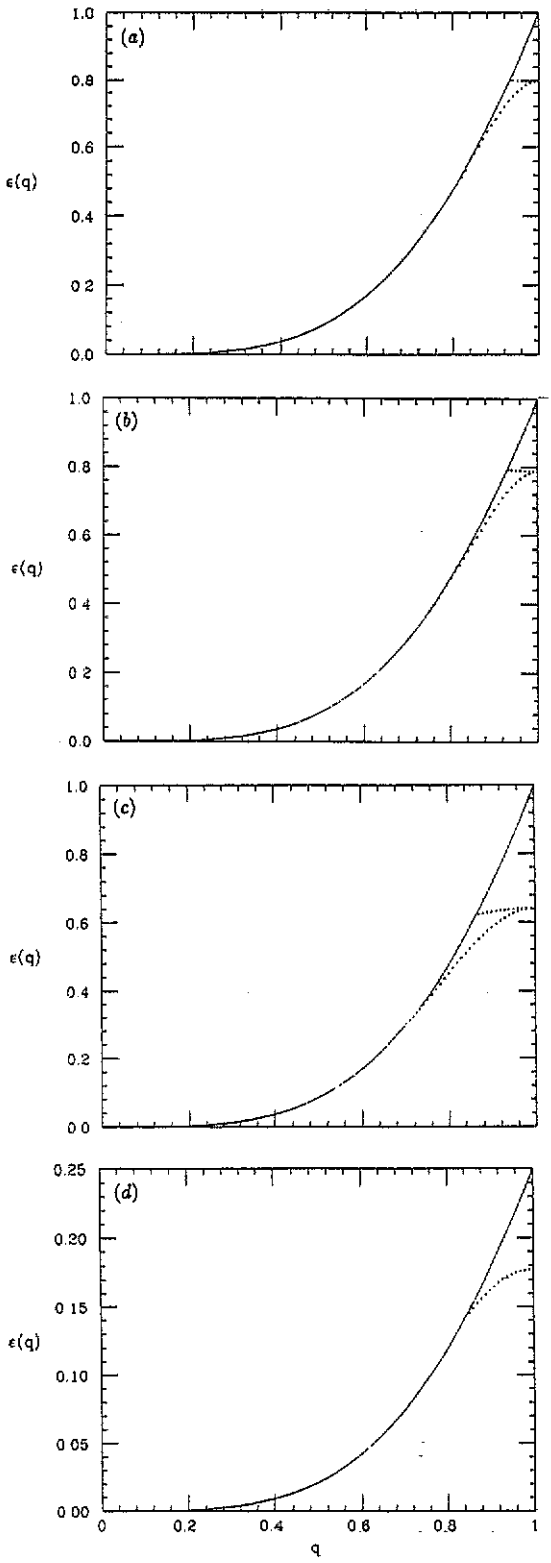

Figure 2. (*a*) Lower bound of the two-magnon band of the 3N model for $j_2 = 0$, $j_3 = -\frac{1}{4}$, $j' = 0.01$ in the $(1,1,0)$ direction (full curve). The broken curve is the bound state energy $\epsilon = \hbar\omega/8J_1S$ as function of the reduced wavevector aq/π. (*b*) The same as for figure 2(*a*) but $j' = 0.001$. (*c*) The same as for figure 2(*a*) but $j_2 = -\frac{1}{4}$, $j_3 = -\frac{1}{8}$. This point is a triple point where the two helical phases H_1 and H_2 merge into the ferromagnetic phase (F) [6]. (*d*) The same as for figure 2(*b*) but the wavevector is along the $(1,0,0)$ direction.

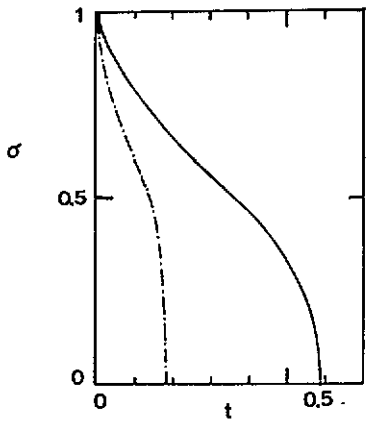

Figure 3. Reduced spontaneous magnetization σ against reduced temperature $t = k_B T/2J_1 S$ in the HF approximation for $j_2 = 0$ and $j_3 = -\frac{1}{4}$: full curve refers to $j' = 0.01$; chain curve refers to $j' = 0.001$.

Within the approximation we have performed the order parameter is

$$\sigma = 1 - \frac{1}{S}\frac{a^2 c}{\pi^3}\int_0^\pi \int_0^\pi \int_0^\pi \mathrm{d}k_x\,\mathrm{d}k_y\,\mathrm{d}k_z \frac{1}{e^{\beta\hbar\omega_k^{(1)}} - 1}. \tag{3.8}$$

The crucial point is that the coefficient of the $k_\perp^2$ contribution in equation (3.2), which is strictly zero at zero temperature on the F–H phase boundary, is restored by thermal fluctuations. We stress that this is a reliable controlled result which clarifies a scenario which differs dramatically from the indication of the linear approach. The order by thermal disorder, suggested in the past for classical systems [11], is now proved for a quantum system.

Let us give the behaviour of the renormalization coefficients ρ for $j_2 = 0$ and $j_3 = -\frac{1}{4}$ at temperatures lower and higher than the inter-plane coupling j'.

$$\rho_1 \simeq \frac{0.04146}{S}\frac{t^{3/2}}{\sqrt{j'}} \qquad \rho' \simeq \frac{0.01931}{S}\frac{t^2}{j'^{3/2}} \tag{3.9}$$

for $t = k_B T/2J_1 S \ll j'$

$$\rho_1 \simeq -\frac{0.05627}{S} t \ln\frac{j'}{t} \qquad \rho' \simeq \frac{0.18786}{S}\left(\frac{t}{j'^{1/2}} - \frac{\sqrt{\pi}}{2}t^{1/2}\right) \tag{3.10}$$

for $t \gg j'$. Moreover $\rho_2 \simeq 2\rho_1$ and $\rho_3 \simeq 4\rho_1$.

Finally we show in figure 3 the order parameter (3.5) plotted against temperature for $j_2 = 0$, $j_3 = -\frac{1}{4}$ and $j' = 0.01$, 0.001. As one can see the LRO is clearly assured but a very peculiar behaviour is seen. The customary $T^{3/2}$ low-temperature behaviour (Bloch's law) shown by a system in the ferromagnetic configuration is dramatically changed. The physical reason is the vanishing of the $k_\perp^2$ coefficient in the SW spectrum for vanishing temperature that causes a sharp low-temperature decrease in the magnetization. At intermediate temperatures the demagnetization slows down because thermal fluctuations support the stability of the system.

The result we have obtained gives some valuable indication about the phase diagram of the model in the neighbourhood of the F–H transition line. The expectation of a disordered phase at any finite temperature for Hamiltonian parameters corresponding to a ferromagnetic ground state has to be definitively ruled out. We stress that the ferromagnetic configuration for the interaction parameters we consider is not simply suggested by the mean field approximation, but it is assured on the basis of an infinite resummation [8] of *all* zero temperature contributions to the ground state energy coming from long wavelength quantum fluctuations within Q^4 where Q is the turn angle between NN spins. In figure 1 we show the phase diagram obtained by the HF approximation in comparison with that obtained by the linear SW theory.

Clearly our approach cannot be extended directly into the helical region because any perturbation approach suffers from dramatic drawbacks when the ground state configuration is not colinear [12], because the SW states become unstable owing to quantum fluctuations around the Goldstone mode corresponding to the classical helix wavevector. So variational approaches have to be invoked [13] but the control of the approximation is lost and exact results cannot be obtained.

4. Summary and conclusions

In this paper we have shown a somewhat rare example of the importance of non-linear effects for the equilibrium configuration of the Heisenberg model. We have considered the so called 3N model where the in-plane exchange interactions extend up to third neighbours. The NN in-plane interaction is ferromagnetic and the inter-plane interaction couples only NN spins. The zero temperature phase diagram in the classical approximation is divided into four regions corresponding to ferromagnetic (F), antiferromagnetic (AF) and two helical (H_1, H_2) configurations [6]. Here we have studied, in particular, the configuration of the model on the F–H transition line at finite temperature. Linear SW theory suggests the absence of LRO because the SW spectrum shows a $k_\perp^4$ dependence in the long wavelength limit instead of the customary quadratic one. This causes a catastrophic number of spin deviations on the basis of the linear SW theory. The critical dimensionality seems to be lowered to $D = 2$ and a disordered phase is expected until zero temperature as illustrated in figure 1. We have tested this result by evaluating in section 2 the two-magnon bound states on the F–H phase boundary because the existence of bound states over the whole Brillouin zone indicates the absence of LRO as one can see when exact results exist. This occurs, for instance, in the one- and two-dimensional ferromagnet with NN interaction [3–5]. The results we obtained shown in figure 2 definitely exclude a two-dimensional-like behaviour of the bound states which indeed do not exist for sufficiently small wavevectors.

In section 3 we solved the question by evaluating the SW energy and the order parameter in the HF approximation that accounts for non-linear contributions at the leading order in $1/S$ and temperature. Notice that in all known cases the HF contribution gives only a slight temperature renormalization of the SW energy and no dramatic effects are found [14]. On the contrary non-linear contributions become dominant on the F–H phase boundary. A temperature-dependent coefficient of $k_\perp^2$ in the SW spectrum is created and this restores LRO. Peculiar features in the spontaneous magnetization appear because the stabilizing $k_\perp^2$ coefficient vanishes with vanishing temperature so that a very steep thermal demagnetization appears in the low temperature region as it is shown in figure 3. Our conclusion about the restoration of

LRO on the F–H line does not contrast with the extension of the Mermin and Wagner theorem we have performed [15] just for the model we have studied here. On the basis of the Bogoliubov inequality we have proved the existence of a surface in the parameter space where the model is disordered at finite temperature. In the present paper we have considered the region of the phase diagram that at zero temperature corresponds to a ferromagnetic configuration so that the surface where no LRO exists has to be searched in the region of helical configuration.

Appendix

In order to perform numerical calculation we replace the sums over the Brillouin zone that appear in equations (2.9) and (2.10) by an integration as follows

$$\frac{1}{N}\sum_{k} f(k) = \frac{1}{(2\pi)^3}\int_{-\pi}^{\pi}\int_{-\pi}^{\pi}\int_{-\pi}^{\pi} \mathrm{d}x\,\mathrm{d}y\,\mathrm{d}z\, f(x,y,z) \tag{A.1}$$

where $x = ak_x$, $y = ak_y$ and $z = ck_z$. As functions of these new variables the denominators of equations (2.9) and (2.10) read

$$\mathrm{d}(\epsilon, q, x, y, z) = \epsilon - \epsilon(q, x, y) - j' + j'\cos(cq_z/2)\cos z \tag{A.2}$$

where

$$\begin{aligned}\epsilon(q,x,y) = {} & 2 - \cos(aq_x/2)\cos x - \cos(aq_y/2)\cos y + 2j_2[1 - \cos(aq_x/2) \\ & \times \cos(aq_y/2)\cos x\cos y - \sin(aq_x/2)\sin(aq_y/2)\sin x\sin y] \\ & + j_3(2 - \cos aq_x\cos 2x - \cos aq_y\cos 2y).\end{aligned} \tag{A.3}$$

The integration over z can be performed analytically. For instance, for D_m and $D_{m,n}$ with $m, n \neq 7$ in which numerators are independent of z, one has

$$\frac{1}{2\pi}\int_{-\pi}^{\pi} \mathrm{d}z \frac{1}{\mathrm{d}(\epsilon, q, x, y, z)} = \mp\frac{1}{D(\epsilon, q, x, y)} \tag{A.4}$$

where

$$D(\epsilon, q, x, y) = \sqrt{[\epsilon - \epsilon(q, x, y) - j']^2 - j'^2\cos^2(cq_z/2)}. \tag{A.5}$$

The upper (lower) sign in equation (A.4) refers to values of ϵ lying below (above) the two-magnon band

$$\epsilon_2 = \epsilon(q, x, y) + j'[1 - \cos(cq_z/2)\cos z]. \tag{A.6}$$

For values of ϵ inside the band the integral (A.4) is zero. Since we are interested in bound states below the two-magnon band we neglect the lower sign in (A.4) and

obtain the following expressions for the D_ms and $D_{m,n}$s

$$D_1 = \frac{1}{(2\pi)^2}\int_{-\pi}^{\pi}\int_{-\pi}^{\pi} dx\,dy \frac{-\cos y}{D(\epsilon,q,x,y)} \tag{A.7}$$

$$D_2 = \frac{1}{(2\pi)^2}\int_{-\pi}^{\pi}\int_{-\pi}^{\pi} dx\,dy \frac{-\cos x}{D(\epsilon,q,x,y)} \tag{A.8}$$

$$D_3 = \frac{1}{(2\pi)^2}\int_{-\pi}^{\pi}\int_{-\pi}^{\pi} dx\,dy \frac{-(\cos x\cos y - \sin x\sin y)}{D(\epsilon,q,x,y)} \tag{A.9}$$

$$D_4 = \frac{1}{(2\pi)^2}\int_{-\pi}^{\pi}\int_{-\pi}^{\pi} dx\,dy \frac{-(\cos x\cos y + \sin x\sin y)}{D(\epsilon,q,x,y)} \tag{A.10}$$

$$D_5 = \frac{1}{(2\pi)^2}\int_{-\pi}^{\pi}\int_{-\pi}^{\pi} dx\,dy \frac{-\cos 2y}{D(\epsilon,q,x,y)} \tag{A.11}$$

$$D_6 = \frac{1}{(2\pi)^2}\int_{-\pi}^{\pi}\int_{-\pi}^{\pi} dx\,dy \frac{-\cos 2x}{D(\epsilon,q,x,y)} \tag{A.12}$$

$$D_7 = \frac{1}{(2\pi)^2}\int_{-\pi}^{\pi}\int_{-\pi}^{\pi} dx\,dy \frac{1}{j'\cos(q_z/2)}\left[1 + \frac{\epsilon - \epsilon(q,x,y) - j'}{D(\epsilon,q,x,y)}\right] \tag{A.13}$$

$$D_{11} = \frac{1}{(2\pi)^2}\int_{-\pi}^{\pi}\int_{-\pi}^{\pi} dx\,dy \frac{-\cos^2 y}{D(\epsilon,q,x,y)} \tag{A.14}$$

$$D_{12} = \frac{1}{(2\pi)^2}\int_{-\pi}^{\pi}\int_{-\pi}^{\pi} dx\,dy \frac{-\cos x\cos y}{D(\epsilon q,x,y)} \tag{A.15}$$

$$D_{22} = \frac{1}{(2\pi)^2}\int_{-\pi}^{\pi}\int_{-\pi}^{\pi} dx\,dy \frac{-\cos^2 x}{D(\epsilon,q,x,y)} \tag{A.16}$$

$$D_{13} = \frac{1}{(2\pi)^2}\int_{-\pi}^{\pi}\int_{-\pi}^{\pi} dx\,dy \frac{-\cos y(\cos x\cos y - \sin x\sin y)}{D(\epsilon,q,x,y)} \tag{A.17}$$

$$D_{14} = \frac{1}{(2\pi)^2}\int_{-\pi}^{\pi}\int_{-\pi}^{\pi} dx\,dy \frac{-\cos y(\cos x\cos y + \sin x\sin y)}{D(\epsilon,q,x,y)} \tag{A.18}$$

$$D_{23} = \frac{1}{(2\pi)^2}\int_{-\pi}^{\pi}\int_{-\pi}^{\pi} dx\,dy \frac{-\cos x(\cos x\cos y - \sin x\sin y)}{D(\epsilon,q,x,y)} \tag{A.19}$$

$$D_{24} = \frac{1}{(2\pi)^2}\int_{-\pi}^{\pi}\int_{-\pi}^{\pi} dx\,dy \frac{-\cos x(\cos x\cos y + \sin x\sin y)}{D(\epsilon,q,x,y)} \tag{A.20}$$

$$D_{33} = \frac{1}{(2\pi)^2}\int_{-\pi}^{\pi}\int_{-\pi}^{\pi} dx\,dy \frac{-(\cos x\cos y - \sin x\sin y)^2}{D(\epsilon,q,x,y)} \tag{A.21}$$

$$D_{34} = \frac{1}{(2\pi)^2}\int_{-\pi}^{\pi}\int_{-\pi}^{\pi} dx\,dy \frac{-(\cos^2 x\cos^2 y - \sin^2 x\sin^2 y)}{D(\epsilon,q,x,y)} \tag{A.22}$$

$$D_{44} = \frac{1}{(2\pi)^2}\int_{-\pi}^{\pi}\int_{-\pi}^{\pi} dx\,dy \frac{-(\cos x\cos y + \sin x\sin y)^2}{D(\epsilon,q,x,y)} \tag{A.23}$$

$$D_{15} = \frac{1}{(2\pi)^2}\int_{-\pi}^{\pi}\int_{-\pi}^{\pi} \mathrm{d}x\,\mathrm{d}y \frac{-\cos y \cos 2y}{D(\epsilon, q, x, y)} \tag{A.24}$$

$$D_{16} = \frac{1}{(2\pi)^2}\int_{-\pi}^{\pi}\int_{-\pi}^{\pi} \mathrm{d}x\,\mathrm{d}y \frac{-\cos y \cos 2x}{D(\epsilon, q, x, y)} \tag{A.25}$$

$$D_{25} = \frac{1}{(2\pi)^2}\int_{-\pi}^{\pi}\int_{-\pi}^{\pi} \mathrm{d}x\,\mathrm{d}y \frac{-\cos x \cos 2y}{D(\epsilon, q, x, y)} \tag{A.26}$$

$$D_{26} = \frac{1}{(2\pi)^2}\int_{-\pi}^{\pi}\int_{-\pi}^{\pi} \mathrm{d}x\,\mathrm{d}y \frac{-\cos x \cos 2x}{D(\epsilon, q, x, y)} \tag{A.27}$$

$$D_{35} = \frac{1}{(2\pi)^2}\int_{-\pi}^{\pi}\int_{-\pi}^{\pi} \mathrm{d}x\,\mathrm{d}y \frac{-\cos 2y(\cos x \cos y - \sin x \sin y)}{D(\epsilon, q, x, y)} \tag{A.28}$$

$$D_{36} = \frac{1}{(2\pi)^2}\int_{-\pi}^{\pi}\int_{-\pi}^{\pi} \mathrm{d}x\,\mathrm{d}y \frac{-\cos 2x(\cos x \cos y - \sin x \sin y)}{D(\epsilon, q, x, y)} \tag{A.29}$$

$$D_{45} = \frac{1}{(2\pi)^2}\int_{-\pi}^{\pi}\int_{-\pi}^{\pi} \mathrm{d}x\,\mathrm{d}y \frac{-\cos 2y(\cos x \cos y + \sin x \sin y)}{D(\epsilon, q, x, y)} \tag{A.30}$$

$$D_{46} = \frac{1}{(2\pi)^2}\int_{-\pi}^{\pi}\int_{-\pi}^{\pi} \mathrm{d}x\,\mathrm{d}y \frac{-\cos 2x(\cos x \cos y + \sin x \sin y)}{D(\epsilon, q, x, y)} \tag{A.31}$$

$$D_{55} = \frac{1}{(2\pi)^2}\int_{-\pi}^{\pi}\int_{-\pi}^{\pi} \mathrm{d}x\,\mathrm{d}y \frac{-\cos^2 2y}{D(\epsilon, q, x, y)} \tag{A.32}$$

$$D_{56} = \frac{1}{(2\pi)^2}\int_{-\pi}^{\pi}\int_{-\pi}^{\pi} \mathrm{d}x\,\mathrm{d}y \frac{-\cos 2x \cos 2y}{D(\epsilon, q, x, y)} \tag{A.33}$$

$$D_{66} = \frac{1}{(2\pi)^2}\int_{-\pi}^{\pi}\int_{-\pi}^{\pi} \mathrm{d}x\,\mathrm{d}y \frac{-\cos^2 2x}{D(\epsilon, q, x, y)} \tag{A.34}$$

$$D_{17} = \frac{1}{(2\pi)^2}\int_{-\pi}^{\pi}\int_{-\pi}^{\pi} \mathrm{d}x\,\mathrm{d}y \frac{\cos y}{j' \cos(cq_z/2)}\left[1 + \frac{\epsilon - \epsilon(q, x, y) - j'}{D(\epsilon, q, x, y)}\right] \tag{A.35}$$

$$D_{27} = \frac{1}{(2\pi)^2}\int_{-\pi}^{\pi}\int_{-\pi}^{\pi} \mathrm{d}x\,\mathrm{d}y \frac{\cos x}{j' \cos(cq_z/2)}\left[1 + \frac{\epsilon - \epsilon(q, x, y) - j'}{D(\epsilon, q, x, y)}\right] \tag{A.36}$$

$$D_{37} = \frac{1}{(2\pi)^2}\int_{-\pi}^{\pi}\int_{-\pi}^{\pi} \mathrm{d}x\,\mathrm{d}y \frac{\cos x \cos y - \sin x \sin y}{j' \cos(cq_z/2)}\left[1 + \frac{\epsilon - \epsilon(q, x, y) - j'}{D(\epsilon, q, x, y)}\right] \tag{A.37}$$

$$D_{47} = \frac{1}{(2\pi)^2}\int_{-\pi}^{\pi}\int_{-\pi}^{\pi} \mathrm{d}x\,\mathrm{d}y \frac{\cos x \cos y + \sin x \sin y}{j' \cos(cq_z/2)}\left[1 + \frac{\epsilon - \epsilon(q, x, y) - j'}{D(\epsilon, q, x, y)}\right] \tag{A.38}$$

$$D_{57} = \frac{1}{(2\pi)^2}\int_{-\pi}^{\pi}\int_{-\pi}^{\pi} \mathrm{d}x\,\mathrm{d}y \frac{\cos 2y}{j' \cos(cq_z/2)}\left[1 + \frac{\epsilon - \epsilon(q, x, y) - j'}{D(\epsilon, q, x, y)}\right] \tag{A.39}$$

$$D_{67} = \frac{1}{(2\pi)^2}\int_{-\pi}^{\pi}\int_{-\pi}^{\pi} \mathrm{d}x\,\mathrm{d}y \frac{\cos 2x}{j' \cos(cq_z/2)}\left[1 + \frac{\epsilon - \epsilon(q, x, y) - j'}{D(\epsilon, q, x, y)}\right] \tag{A.40}$$

$$D_{77} = \frac{1}{(2\pi)^2}\int_{-\pi}^{\pi}\int_{-\pi}^{\pi} \mathrm{d}x\,\mathrm{d}y \frac{\epsilon(q, x, y) + j' - \epsilon}{j'^2 \cos^2(cq_z/2)}\left[1 + \frac{\epsilon - \epsilon(q, x, y) - j'}{D(\epsilon, q, x, y)}\right]. \tag{A.41}$$

For directions of high symmetry as, for instance $(1,1,0)$, the number of independent D_ms and $D_{m,n}$s reduces noticably. In particular for $j_2 = 0$, $j_3 > -\frac{1}{4}$ and for small j', the zeros of the determinant (2.8) are the solutions of the two following equations

$$\left(1 - \frac{1}{2S} I_{1a}\right)\left(1 - \frac{j_3}{2S} I_{3a}\right) - \frac{j_3}{4S^2} I_{3c}^2 = 0 \tag{A.42}$$

$$\left(1 - \frac{1}{2S} I_{1b}\right)\left(1 - \frac{j_3}{2S} I_{3b}\right) - \frac{j_3}{4S^2} I_{3d} I_{3e} = 0 \tag{A.43}$$

$$I_{1a} = \frac{1}{\pi^2}\int_0^\pi \int_0^\pi \mathrm{d}x\,\mathrm{d}y \frac{\cos x(\cos x - \cos y)}{\sqrt{A^2(\epsilon,q,x,y) - j'^2}} \tag{A.44}$$

$$I_{1b} = \frac{1}{\pi^2}\int_0^\pi \int_0^\pi \mathrm{d}x\,\mathrm{d}y \frac{\cos x[\cos x + \cos y - 2\cos(aq/2)]}{\sqrt{A^2(\epsilon,q,x,y) - j'^2}} \tag{A.45}$$

$$I_{3a} = \frac{1}{\pi^2}\int_0^\pi \int_0^\pi \mathrm{d}x\,\mathrm{d}y \frac{\cos 2x(\cos 2x - \cos 2y)}{\sqrt{A^2(\epsilon,q,x,y) - j'^2}} \tag{A.46}$$

$$I_{3b} = \frac{1}{\pi^2}\int_0^\pi \int_0^\pi \mathrm{d}x\,\mathrm{d}y \frac{\cos 2x(\cos 2x + \cos 2y - 2\cos aq)}{\sqrt{A^2(\epsilon,q,x,y) - j'^2}} \tag{A.47}$$

$$I_{3c} = \frac{1}{\pi^2}\int_0^\pi \int_0^\pi \mathrm{d}x\,\mathrm{d}y \frac{\cos x(\cos 2x - \cos 2y)}{\sqrt{A^2(\epsilon,q,x,y) - j'^2}} \tag{A.48}$$

$$I_{3d} = \frac{1}{\pi^2}\int_0^\pi \int_0^\pi \mathrm{d}x\,\mathrm{d}y \frac{\cos x(\cos 2x + \cos 2y) - 2\cos 2x\cos(aq/2)}{\sqrt{A^2(\epsilon,q,x,y) - j'^2}} \tag{A.49}$$

$$I_{3e} = \frac{1}{\pi^2}\int_0^\pi \int_0^\pi \mathrm{d}x\,\mathrm{d}y \frac{\cos x(\cos 2x + \cos 2y - 2\cos aq)}{\sqrt{A^2(\epsilon,q,x,y) - j'^2}} \tag{A.50}$$

where

$$A(\epsilon,q,x,y) = 2 - \cos(aq/2)(\cos x + \cos y) + 2j_3[1 + \cos aq(1 - \cos^2 x - \cos^2 y)] + j' - \epsilon \tag{A.51}$$

and

$$\epsilon < 2\left(1 - \cos\frac{aq}{2}\right)\left[1 + 2j_3\left(1 + \cos\frac{aq}{2}\right)\right]. \tag{A.52}$$

Notice that I_{1a}, I_{3a} and I_{3c} are regular even for $j' = 0$ and the bound state corresponding to the solution of (A.42) exists only near the zone boundary. For $j_3 = -\frac{1}{4}$, $j' = 0.01$ and $j' = 0.001$ this bound state merges into the two-magnon band at $q = 0.933\pi/a$ and $q = 0.930\pi/a$, respectively. In contrast I_{1b}, I_{3b}, I_{3d} and I_{3e} are logarithmically divergent for $j' \to 0$. This implies that (A.43) has a solution over an increasing portion of the Brillouin zone until the whole Brillouin zone is covered at $j' = 0$. For $j' = 0.01$ and $j' = 0.001$ this bound state merges into the two-magnon band at $q = 0.810\pi/a$ and $q = 0.731\pi/a$, respectively. Notice that even if the lower bound of the two-magnon band shows a peculiar q^4 behaviour at long wavelengths

$$\epsilon_2(q,0,0) = \frac{1}{2}\left(1 - \cos\frac{aq}{2}\right)^2 \tag{A.53}$$

the integrals involved in (A.43) do not show any anomalous behaviour.

References

[1] Mattis D 1965 *The Theory of Magnetism* (New York: Harper and Row)
[2] Dyson F J 1956 *Phys. Rev.* **102** 1217
[3] Landau L 1958 *Statistical Physics* (New York: Pergamon)
[4] Mermin N D and Wagner H 1966 *Phys. Rev. Lett.* **17** 1133
[5] Wortis M 1963 *Phys. Rev.* **132** 85
[6] Rastelli E, Tassi A and Reatto L 1979 *Physica* B **97** 1
[7] Harris A B and Rastelli E 1987 *J. Phys. C: Solid State Phys.* **20** L741
[8] Harris A B, Pimpinelli A, Rastelli E and Tassi A 1989 *J. Phys.: Condens. Matter* **1** 3821
[9] Rastelli E, Reatto L and Tassi A 1983 *J. Phys. C: Solid State Phys.* **16** L331
[10] Chandra P and Doucot B 1988 *Phys. Rev.* B **38** 9335
[11] Villain J, Bideaux R, Carton J P and Conte R 1980 *J. Physique* **41** 1263
Hanley C L 1989 *Phys. Rev. Lett.* **62** 2056
[12] Rastelli E, Reatto L and Tassi A 1985 *J. Phys. C: Solid State Phys.* **18** 353
[13] Rastelli E and Tassi A 1986 *J. Phys. C: Solid State Phys.* **19** 1993
[14] Bloch M 1962 *Phys. Rev. Lett.* **9** 286
[15] Rastelli E and Tassi A 1989 *Phys. Rev.* B **40** 5282